Charge Neutralization of Aersol Carbon Nanofibers

Charge Neutralization of Aerosol Carbon Nanofibers

Yutaka TANAKA[1], Hidenori HIGASHI[2], Eric MANIRAKIZA[2], Takafumi SETO[2], Yoshio OTANI[2] and Makoto HIRASAWA[3]

[1]*Tokyo Dylec Corp., Naito-machi 1, Shinjuku-ku, Tokyo 160-0014, Japan*

[2]*School of Natural System, Kanazawa University, Kakuma-machi, Kanazawa 920-1192, Japan*

[3]*National Institute of Advanced Industrial Science and Technology (AIST), Namiki 1-2-1, Tsukuba 305-8564, Japan*

Charging characteristics of carbon nanofibers (CNFs) with a 241-Am charge neutralizer were investigated using diameter- and length-controlled CNF particles, which were generated by a floating catalyst CVD method. The neutral fraction and charge distribution of CNF measured by aerosol techniques suggested that the fraction of neutral particles is much lower than that predicted by the conventional charging theory for spherical particles and that there exist a large number of multiply charged particles in charge equilibrium. Furthermore, it was found that the charge equivalent diameter that is twice the one proposed in a previous work gives a good prediction for the charge distribution of CNF with a diameter smaller than 20 nm and aspect ratio between 5 and 40.

Introduction

Fibrous particles in nanometer size (nanofibers) such as carbon nanofibers (CNF), carbon nanotubes (CNT) or semiconductor nanowires are promising new functional materials and their applications have been anticipated in various fields. Measurement of airborne nanofibers is important not only for the quality control of nanoparticles in gas-phase synthesis, but also for the prevention of worker exposure to CNF in the manufacturing environment since the adverse health effects of CNF are still uncertain. A differential mobility analyzer (DMA) is one of the most effective devices in classifying nanoparticles and measuring the size distribution. However, the application of a DMA to the size distribution measurement of CNF is not well-established because of the complex behavior of CNF in the classification column (Kim *et al.*, 2007). In addition, the charging characteristics of CNF are not well understood, although it is an important process in the pretreatment of classification.

The charging of spherical aerosol particles is a well known process in which the charging mechanism depends on the diameter of the sphere. In the nanometer size range, the dominant charging process is diffusion charging, and the charging efficiency can be obtained as a function of particle size (e.g., Adachi *et al.*, 1985). There are several reports on the charging efficiency for submicron fibrous particles (Wen *et al.*, 1984a, 1984b), but the applicability of the charging theory to fibrous particles of nanometer diameter has not yet been well examined. As for the charging characteristics of CNTs, Kulkarni *et al.* (2009) investigated the equilibrium charge distribution of agglomerated single walled CNTs with an aspect ratio of about 3. They reported that the fraction of neutral particles (neutral fraction) is much lower than the neutral fraction predicted by the theory for spherical particles, suggesting the higher charging probability of the CNT. However, their CNTs were not in the form of single fibers, but agglomerates, and the size range was over 300 nm in electrical mobility diameter because they aerosolized an aqueous CNT suspension by an ultrasonic nebulizer or Couette flow generator. Seto *et al.* (2010) also generated fibrous aerosol (aspect ratio; 20–37) by atomizing aqueous suspensions of multi-walled CNT. They reported that the DMA-classified fibrous particles contain a significant amount of multiply charged CNTs which have a significant influence on the filtration efficiencies. More recently, Ku *et al.* (2011) generated a high-aspect ratio aerosol by a vortex generator and investigated the bipolar charging characteristics of these fibers. They employed charge-equivalent diameter and surface area

equivalent diameter as characteristic dimensions of fibrous aerosol. However, the experimentally measured neutral fraction of fibrous particles was still lower than the predicted one. Therefore, there is a limit in conventional charging theory in predicting the charging process of high aspect-ratio fibrous particles in nanometer size.

In order to clarify the charging process of nanometer-sized fibrous particles, it is essential to establish a method for generating test particles of uniform diameter and length. As mentioned above, nebulization of an aqueous suspension or mechanical dispersion using shear flow is rather difficult in the aspect of obtaining isolated fibers because of high adhesion force and tangling of fibers. As a result, most of the test particles were agglomerates (for example, Kulkarni *et al.*, 2009) and isolated but limited to large sizes (Seto *et al.*, 2010). On the other hand, direct synthesis of carbon nanotubes by an aerosol process such as catalyst-assisted chemical vapor deposition (CVD) is a candidate for generating test nanofibers if non-agglomerated state in the gas phase. Among the several methods (for example, laser ablation, Klanwan *et al.*, 2010; catalyst CVD, Tian *et al.*, 2011), the combination of DMA and CVD is one of the most suitable methods to generate test particles with uniform diameter and length (Kim and Zachariah, 2006). With this method, the CNF diameter was controlled by the classification of catalyst particles in the first DMA. After the CVD-growth of CNFs with uniform diameter, the products were classified according to length by the second DMA. The biggest advantage of this method is that we can control the charge of the CNF with the same diameter but different lengths to a 'single' charge. The catalyst particles introduced to the bipolar charger are so small that they cannot retain more than a single charge at a bipolar charge equilibrium, and CNFs grow on the catalysts while keeping the single charge. In the present study, we synthesized CNF with a method similar to the one developed by Kim and Zachariah (2006), and applied it to obtain basic data on bipolar charging characteristics of CNF aerosol.

1. Experimental

1.1 Method for generating test particles

A monodispersed CNF aerosol was generated by a floating catalyst CVD method similar to the one developed by Kim and Zachariah (2006). Catalytic Ni nanoparticles were generated by laser ablation of Ni target in nitrogen gas, and introduced to the first DMA after bipolar charging with 241-Am neutralizer. Since Ni nanoparticles were smaller than 20 nm in diameter, they consisted mostly of neutral particles with a small fraction of singly charged particles. Therefore, after the classification with DMA, only singly-charged monodispersed Ni nanoparticles were introduced to a tubular reactor and mixed with acetylene and hydrogen. CNFs grew due to the surface reaction of carbon precursors on the Ni catalyst to form CNFs with uniform diameter but different lengths. Then, the CNFs were classified according to the length by the second DMA to obtain CNFs with uniform diameter and lengths.

Typical TEM images of CNF particles generated by the floating catalyst CVD method are shown in **Figure 1**. CNFs were generated using the catalyst nanoparticles with diameters of 10 and 15 nm. As seen in Figure 1, although CNFs have curvature, the diameter is almost uniform and increases with the catalyst particle diameter. CNFs with similar structures were reported by Kim and Zachariah (2006). The curvatures and twisting of fibers may be caused the lattice mismatch and the introduction of defects during rapid CVD growth. Some thinner CNFs in Figure 1 may be caused by the breakage of agglomerated catalytic particles during the growth.
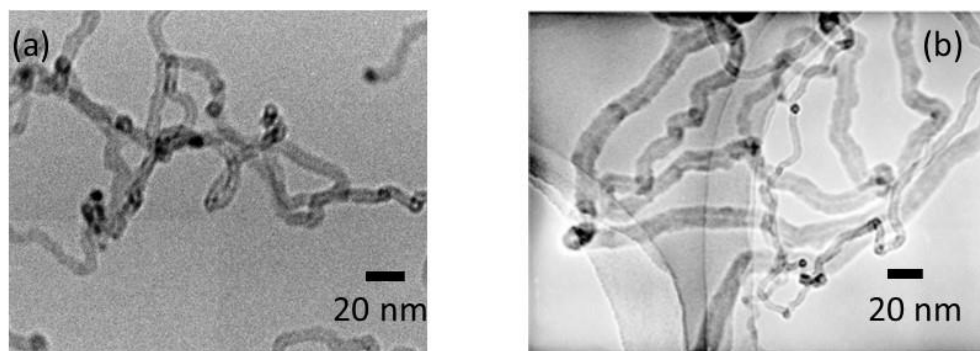

Fig. 1 Transmission electron micrographs of CNFs generated by the vapor phase growth on size-selected catalyst particles, (a) CNFs grown on 10-nm Ni particles and (b) those grown on 15-nm Ni particles

Table 1 Characteristic dimensions of CNF used in the present work

Catalyst diameter D_{Cat} [nm]	CNF diameter D_{CNF} [nm]	CNF length L_{CNF} [nm]	Aspect ratio β [-]	Mobility diameter D_m [nm]
10	7.1	77–280	10.8–39.4	20–50
15	10.7	51–186	4.8–17.4	20–50
20	14.2	65–243	4.6–17.1	30–70
25	17.8	112–300	6.3–16.9	50–90

We measured the CNF diameter and length by TEM and obtained empirical correlation equations giving the relationships between Ni catalyst particle diameter and CNF diameter and those between the CNF length and the electrical mobility equivalent diameter (see Appendix).

$$D_{CNF} = 0.71 D_{Cat} + 0.02 \qquad (1)$$

$$L_{CNF} = \frac{\pi}{4} \frac{(0.80 D_m + 10.33)^2}{D_{CNF}} \qquad (2)$$

Here, D_{CNF} is the CNF diameter, D_{Cat} is the Ni catalytic particle diameter, L_{CNF} is the CNF length and D_m is the mobility equivalent diameter. These correlation equations were those obtained for 10 nm < D_{Cat} < 25 nm, 42 nm < D_m < 180 nm, 3.6 nm < L_{CNF} < 8.1 mm. **Table 1** shows the dimensions of CNFs calculated by the empirical equations for the present experiments.

1.2 Measurement of charging efficiency

Singly-charged (negative) CNFs with uniform diameter and length, which were obtained by the method described in the previous section, were used to study the charging characteristics of CNFs with bipolar ions. After passing uniform CNF particles through a 241-Am bipolar charger (AM-241 : α-radiation source, 3 MBq, 38 mm I.D., 158 mm length, Tokyo Dylec Corporation), we measured (a) the neutral fraction and (b) the distribution of the number of charges using the experimental system shown in **Figure 2**. The particles were stably supplied at a number concentration less than 1000 particles cm⁻³ and the ion concentration was about 10^{11}–10^{13} m⁻³. For comparison, we also used monodispersed sodium chloride particles (singly-charged, negative) generated by an evaporation-condensation method. The neutral fraction was obtained as the ratio of the number of uncharged particles to the total number of particles by using the path (a) shown in Figure 2. With this path, we introduced particles from the charge neutralizer into an electrostatic precipitator (ESP), and measured the number concentrations with and without applying voltage to the ESP (N_{ON}, N_{OFF}) using a condensation particle counter (CPC, Model 3022, TSI Inc.). Diffusional deposition loss in the ESP for 10-nm particles predicted by the Gormley and Kennedy equation (1949) was about 3%. The CNFs used in the present work were larger than 50 nm in mobility equivalent diameter so that the loss in the ESP was negligibly small. The particle number concentrations with and without applying voltage were determined by averaging ten consecutive readings of CPC, and this procedure was repeated three times. The neutral fraction was calculated by the following equation.

$$f(v) = 1 - \frac{N_{ON}}{N_{OFF}} \qquad (3)$$

Here, we kept the aerosol flow rate through the charger constant at 1.5 L min⁻¹ (the mean residence time in the charger was about 10 s). When the ion concentration is sufficiently high compared to the particle concentration and the charging time is adequately long, the charging state of particles becomes the equilibrium charge distribution. Wiedensohler (1988) derived the following approximation equation for the charge distribution of particles based on Fuchs's theorem (1963).
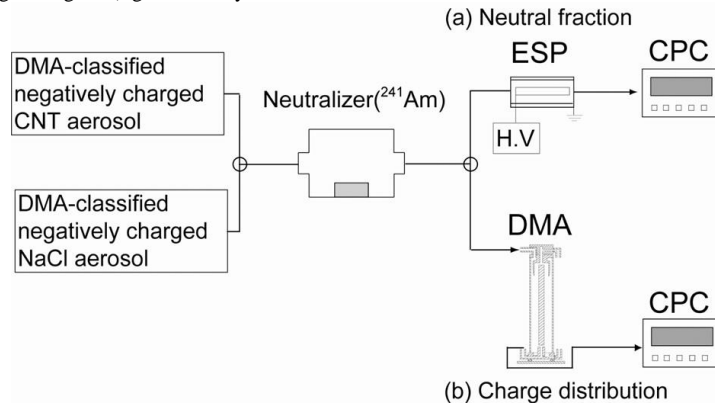
Fig. 2 Experimental setup for the measurements of neutral fraction and charge distribution

$$f(v, D_{p}) = 10^{\sum_{i=0}^{5} a_i(v) \times (\log D_p)^i} \qquad (4)$$

Here, v is the number of elementary charge units on a particle, and $a_i(v)$'s are the coefficients given by Wiedensohler (1988). Eq. (4) is valid for the particle size range: 1 nm $\leqq D_p \leqq$ 1000 nm for v = -1, 0, 1; and 20 nm $\leqq D_p \leqq$ 1000 nm for v = -2, 2. He assumed that the concentrations for positive and negative ions were equal and the ratio of ion mobilities was 0.875.

The measurement of charge number distribution was carried out using the path (b) shown in Figure 2 where third DMA was employed. For monodispersed particles, the peaks of multiply charged particles appear discretely over the electrical mobility depending on the number of charges. The details will be discussed in the next section.

2. Results and Discussion

2.1 Neutral fractions

Figure 3 shows the neutral fractions as a function of electrical mobility equivalent diameter of CNF particles. The solid lines are the theoretical neutral fraction for the spherical particles predicted by Eq. (4), in which D_p is assigned as the mobility equivalent diameter. Although the neutral fraction of spherical sodium chloride particles is slightly lower than the predicted, the experimental data show the same dependency on particle size as the predicted line. The small deviation of experimental data from the prediction may be attributed to the fact that the NaCl particles used in the present experiment were not completely spherical in shape, i.e. agglomerates.
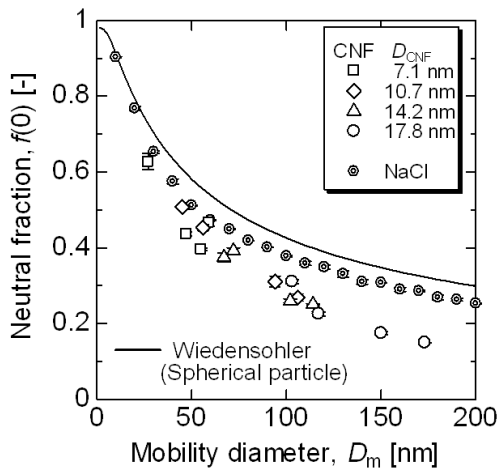
Since spherical particles have the smallest collision probability with ions compared to the irregular-shaped particles with the same projected area, non-spherical particles would be more easily charged than spherical particles. Therefore, the neutral fraction $f(0)$ of agglomerated NaCl particles is smaller than that of the spherical particles.

The neutral fractions of CNFs are considerably lower than the predicted, and we cannot see a clear difference in neutral fraction due to the CNF diameter, D_{CNF}, when the electrical mobility equivalent diameter of CNF is the same. Therefore, we can infer that CNFs have more charged fractions than spherical particles at the charge equilibrium.

2.2 Distribution of number of charges on a particle

The mobility distribution of CNF (the diameter of CNF is D_{CNF} = 17.8 nm, and the electrical mobility diameter is 140 nm for singly-charged particle at Z_p = 1.1×10^{-8} m^2 V^{-1} s^{-1}) after bipolar charging is shown in **Figure 4**. The numbers in Figure 4 show the number of elementary charges and the minus sign designates negatively charged particles. In Figure 4, the highest peak of electrical mobility appears at the electrical mobility nearly equal to that of singly-charged particles (Z_p/Z_{pi} = 1), implying that the largest fraction of charged CNF consists of singly-charged particles. In this figure, we also see many other peaks of multiply-charged particles at the electrical mobility approximately doubled, tripled, and so forth, implying that the mobility-classified CNFs of uniform fiber diameter contain many multiply-charged fractions.
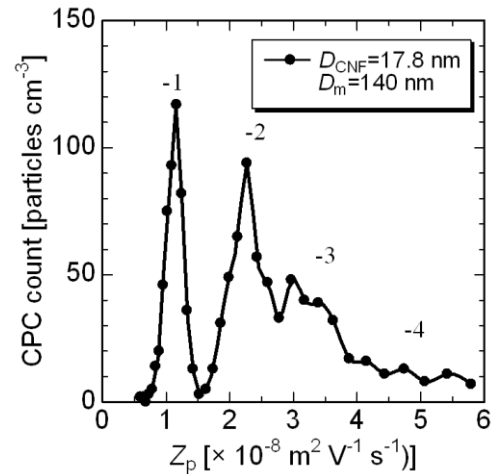

Fig. 3 Neutral fractions of CNFs and NaCl particles

Fig. 4 DMA spectrum of size-selected CNF aerosol (D_m = 140 nm) after passing through a charge neutralizer for negatively charged particles

In order to evaluate the abundance of multiply-charged fractions, the peak ratios (i.e. number ratios) of doubly-charged particles to singly-charged particles for negatively charged particles are plotted in **Figure 5** with the CNF diameter as a parameter. The solid line in the figure is the theoretical line for spherical particles predicted by Eq. (4). The ratio of doubly- to singly-charged particles for spherical sodium chloride particles is higher than the theoretical line, because the fraction of neutral particles are smaller than the predicted as mentioned in Figure 3. In Figure 5, we see that the ratio of doubly- to singly-charged CNFs is considerably larger than those predicted by Eq. (4) and about twice those of spherical NaCl particles. We also find that there is no clear difference in the doubly- to singly- charge particle number ratio according to the CNF diameter when the electrical mobility equivalent diameter of CNFs is the same. The no clear dependence of doubly- to singly-charged particle ratio on CNF diameter for the CNF studied in the present work ($7.1 < D_{CNF} < 17.8$ nm, $51 < L_{CNF} < 300$ nm; shown in Table 1) may be explained as follows. For the classification of CNF with DMA, we must take into account the particle orientation in the DMA column and the positions of electrical charges on a CNF particle, as discussed by Kim *et al.* (2007). Since the electrical mobility is proportional to the projected area of CNF in the direction to the particle's movement, a thinner CNF with a given mobility has a larger length to give the same projected area of a thicker CNF with the same mobility, provided that the orientations of CNFs with different diameters are the same in the DMA column. Since the surface area of CNF is proportional to the projected area, the equilibrium charge acquired by CNF is determined roughly by the mobility diameter of CNF.
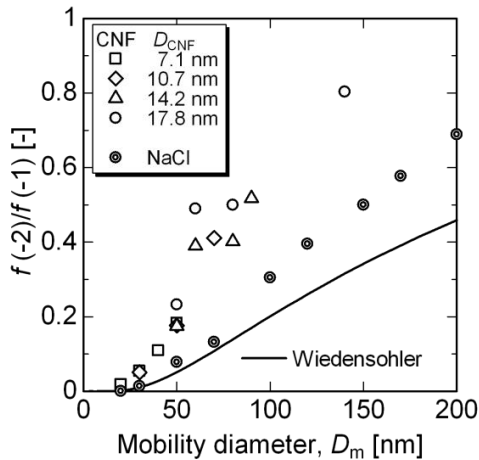

Fig. 5 Number ratios of doubly- to singly- charged particles for negatively charged particles

2.3 Application of charging model to fibrous particles

Wen *et al.* (1984a, 1984b) introduced the following charge equivalent diameter for Boltzmann charge distribution, D_{QE}, in the prediction of charging efficiency of linear chain aggregates by assuming that the aggregates are conducting prolate spheroid in shape.

$$D_{QE} = \frac{d_1 \beta}{\ln(2\beta)} \qquad (5)$$

Here, β is the aspect ratio and d_1 is the length of the minor axis of the spheroid. Wen *et al.* (1984b) used Eq. (5) for predicting the average charge and electrical mobility distribution of linear chain aggregates (primary particle size: $d_1 = 41$ and 81 nm, and the number of primary particles in the aggregate: $\beta = 10$-200) and found that Eq. (5) could give a good prediction of electrical mobility distribution within about 10%, but that it must be doubled or tripled to give the required level of average charge.

In **Figure 6**, according to the finding by Wen *et al.* (1984a), the experimental neutral fractions are plotted against twice the charge equivalent diameter of D_{QE} which was calculated by the diameter and length of CNFs given in Table 1.

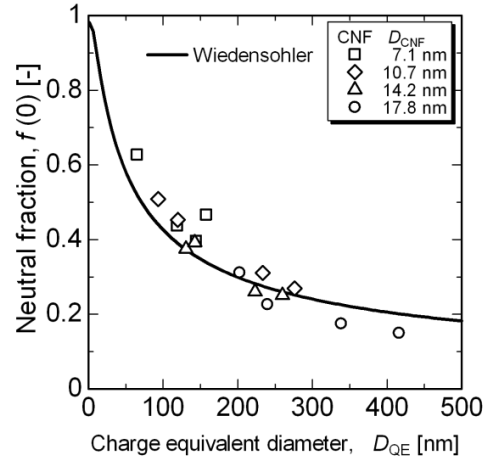$$D_{QE} = \frac{2d_1 \beta}{\ln(2\beta)} \qquad (6)$$

Fig. 6 Neutral fraction of CNF plotted against charge equivalent diameter

As seen in Figure 6, by introducing doubled D_{QE} given by Eq. (6) rather than Eq. (5) or the electrical mobility equivalent diameter, the agreement between the experimental data and the prediction is quite good. **Figure 7** shows the ratios of doubly- and singly-charged particles as a function of doubled charge equivalent diameter. As seen in this figure, the agreement

between the experiment and the prediction is very good. Wen *et al.* (1984a, 1984b) did not give verification for introducing the doubled D_{QE}, but this correction works very well even for the CNF with a diameter less than 20 nm studied in the present work. Ku *et al.* (2011) and Kulkarni *et al.* (2009) also reported that the charge equivalent diameter suggested by Wen *et al.* (1984a, 1984b) well represented the charging characteristics of fiber aerosols, but that the agreement with the prediction was not satisfactory for fibers with large aspect ratios. It seems that, for a longer fiber, the electrical charge on a fiber may exist more stably because the charge can be localized at the edges of a long fiber.
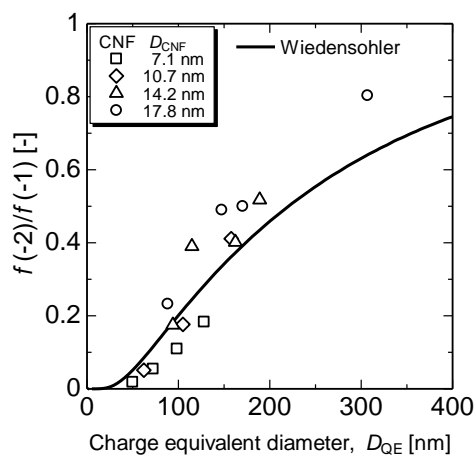

Fig. 7 Number ratios of doubly- to singly- charged particles plotted against charge equivalent diameter

Conclusions

We have measured the charged fractions of fibrous particles by bipolar charging using CNFs with nanometer-order diameter, and found that the fraction of neutral particles was much lower than that predicted by the conventional theory for spherical particles and that there existed a large number of multiply-charged particles in charge equilibrium. Therefore, when we measure the particle size distribution of nanometer-sized fibrous particles using bipolar charging followed by an electrical mobility classification, the inclusion of multiply-charged particles influences the retrieved size distribution more severely than the spherical particles. Furthermore, we found that a charge equivalent diameter that is twice the one suggested by Wen *et al.* (1984a, 1984b) gives a good prediction for the charge distribution of CNF with a diameter smaller than 20 nm and an aspect ratio between 5 and 40. Future work is required to verify the introduction of doubled charge equivalent diameter.

Nomenclature

a_i	= coefficients	[-]
D	= diameter	[m]
d_1	= length of minor axis of spheroid	[m]
f	= fraction of charged particles	[-]
L	= length	[m]
N	= number concentration	[m^{-3}]
Z_p	= electrical mobility	[m^2 s^{-1} V^{-1}]
β	= aspect ratio	[-]
ν	= number of charges	[-]

\<Subscripts\>

Cat	= catalyst
CNF	= carbon nanofiber
m	= mobility
ON	= with applying voltage to ESP
OFF	= without applying voltage to ESP
P	= particle
QE	= charge equivalent

Literature sited

Adachi, M., Y. Kousaka and K. Okuyama; "Unipolar and Bipolar Diffusion Charging of Ultrafine Aerosol Particles," *J. Aerosol Sci.*, **16**, 109–123 (1985)

Fuch, N. A.; "On the Stationary Charge Distribution on Aerosol Particles in a Bipolar Ionic Atmosphere," *Geofisica Pura e Applicata*, **56**, 185–193 (1963)

Gormley P. G. and M. Kennedy; "Diffusion from a Stream Flowing through a Cylindrical Tube," *Proc. Royal Irish Acad.*, **52A**:163–169 (1949)

Kim, S. H., G. W. Mulholland and M. R. Zachariah; "Understanding Ion-mobility and Transport Properties of Aerosol Nanowires," *J. Aerosol Sci.*, **38**, 823–842 (2007)

Kim, S. H. and M. R. Zachariah; "In-flight Kinetic Measurements of the Aerosol Growth of Carbon Nanotubes by Electrical Mobility Classification," *J. Phys. Chem. B*, **110**, 4555–4562 (2006)

Klanwan, J., T. Seto, T. Furukawa, Y. Otani, T. Charinpanitkul, M. Kohno and M. Hirasawa; "Generation and Size Classification of Single-Walled Carbon Nanotube Aerosol Using Atmospheric Pressure Pulsed Laser Ablation (AP-PLA)," *J. Nanoparticle Res.*, **12**, 2747–2755 (2010)

Ku, B. K., G. J. Deye, P. Kulkarni and P. A. Baron; "Bipolar Diffusion Charging of High-aspect Ratio Aerosols," *J. Electrostatics*, **69**, 641–647 (2011)

Kulkarni, P., G. J. Deye and P. A. Baron; "Bipolar Diffusion Charging Characteristics of Single-wall Carbon Nanotube

Aerosol Particles," *J. Aerosol Sci.*, **40**, 164–179 (2009)

Seto T., T. Furukawa, Y. Otani, K. Uchida and S. Endo; "Filtration of Multi-walled Carbon Nanotube Aerosol by Fibrous Filters," *Aerosol Sci. Technol.*, **44**, 734–740 (2010)

Tian, Y., M. Y. Timmermans, M. Partanen, A. G. Nasibulin, H. Jiang, Z. Zhu and E. I. Kauppinen; "Growth of Single-walled Carbon Nanotubes with Controlled Diameters and Lengths by an Aerosol Method," *Carbon*, **49**, 4636–4643 (2011)

Wen, H. Y., G. P. Reischl and G. Kasper; "Bipolar Diffusion Charging of Fibrous Aerosol Particles-I. Charging Theory," *J. Aerosol Sci.*, **15**, 89–101 (1984a)

Wen, H. Y., G. P. Reischl and G. Kasper; "Bipolar Diffusion Charging of Fibrous Aerosol Particles—II. Charge and Electrical Mobility Measurements on Linear Chain Aggregates," *J. Aerosol Sci.*, **15**, 103–122 (1984b)

Wiedensohler, A.; "An Approximation of the Bipolar Charge Distribution for Particles in the Submicron Size Range," *J. Aerosol Sci.*, **19**, 387–389 (1988)

Appendix

The empirical correlation equations of Eqs. (1) and (2) were derived from the relationships between Ni catalyst particle diameter and CNF diameter and those between the CNF length and the electrical mobility equivalent diameter. Isolated CNFs, as shown in **Figure A1**, were chosen to obtain the diameter and length of the CNFs. D_{CNF} was measured at several positions of a CNF from an SEM image and L_{CNF} was measured by sectioning the CNF with straight lines in the SEM image as shown in Figure A1. D_{CNF} and L_{CNF} were averaged for more than 200 particles and the geometric standard deviations were about 1.2-1.4 for D_{CNF}.

The relationship between D_{CNF} and D_{Cat} shown in **Figure A2** is given by Eq. (A1).

$$D_{CNF} = 0.71 D_{Cat} + 0.02 \qquad (A1)$$

The mobility diameter is a function of the projected area. The projected area equivalent diameters D_{prj} calculated by Eq. (A2) are plotted as a function of D_m in **Figure A3**, which gave the correlation equation of Eq. (A3).

$$\frac{\pi}{4} D_{prj}^2 = D_{CNF} L_{CNF} \qquad (A2)$$

$$D_{prj} = 0.80 D_m + 10.33 \qquad (A3)$$

By substituting Eqs. (A1) and (A3) into Eq. (A2), L_{CNF} is given by Eq. (A4).

$$L_{CNF} = \frac{\pi}{4} \frac{(0.80 D_m + 10.33)^2}{0.71 D_{Cat} + 0.02} \qquad (A4)$$
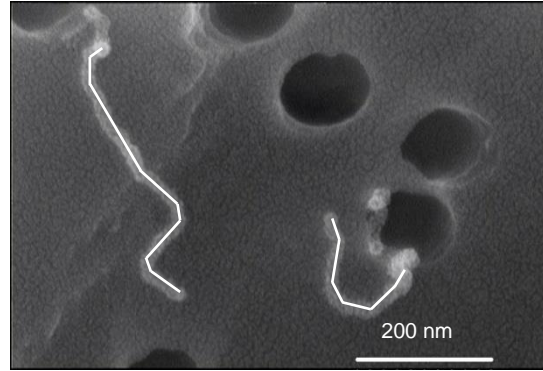
Fig. A1 Determination of L_{CNF} for isolated CNF by SEM image

$$D_{CNF} = 0.71\ D_{Cat} + 0.02$$
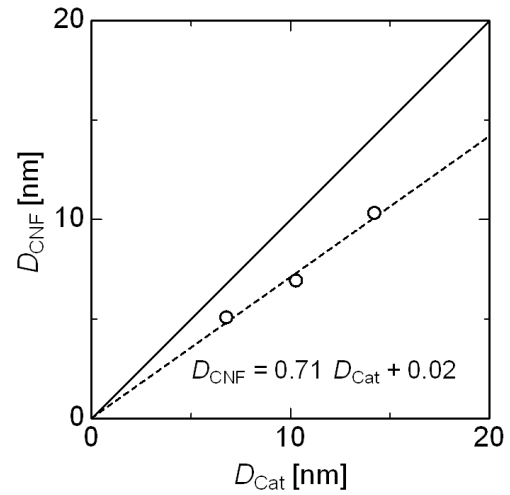
Fig. A2 Relationship of catalyst diameter and CNT diameter
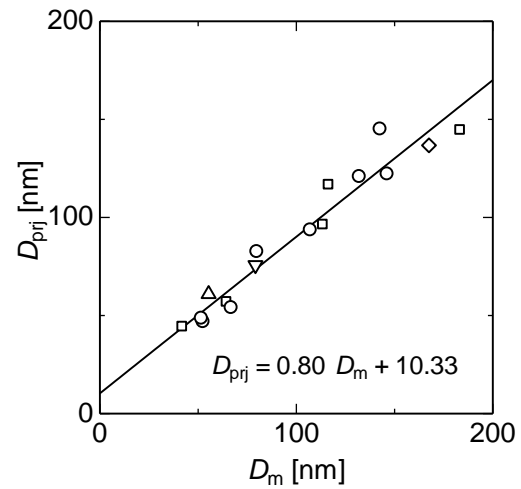

$$D_{prj} = 0.80\ D_m + 10.33$$

Fig. A3 Relationship of mobility diameter and projected diameter